

AN ENRICHED PARTICLE BEAM USING SUPERCONDUCTING RF DEFLECTORS*

H.N. Brown
Brookhaven National Laboratory
Upton, New York

Although many in the audience are closely associated with work in high energy physics, there are others who are concentrating more on the physics of superconductors per se, and so it seems appropriate to review briefly the problem of particle separation as it is encountered in high energy physics experiments.

I. IDENTIFICATION AND SEPARATION OF PARTICLE TYPES

When produced at the target of an accelerator, a beam of secondary particles, directed into the apparatus of a high energy physics experiment, contains several different types of particles. Usually, the experiment concerns the interaction of one particular type (at a given momentum) with the nuclei of a secondary target placed in the beam. These particles differ from one another in numerous characteristics, but unfortunately many of these differences are manifested only in ways which are destructive of the particles themselves. Therefore, the solution to the problem of identifying different particle types in the beam boils down to a determination of the mass of the particle. This is done, indirectly, from the relation $p = m_i v_i$. For the given momentum, a velocity determination yields the mass m_i . Difficulties arise at high momenta, for then this relation becomes

$$p = \frac{m_i v_i}{\sqrt{1 - (v_i/c)^2}}$$

from which

$$\frac{1}{v_i} = \frac{1}{c} \sqrt{1 + \left(\frac{m_i c}{p}\right)^2}$$

and hence, when $p \gg m_i c$, v_i is only slightly different for two different particles whose rest masses m_i have a large relative difference. Nevertheless, these small differences in velocity can be detected (e.g., by time-of-flight measurements or Cerenkov counters) and used to identify particle types in flight. However, in a particle beam which may contain 100 times as many π -mesons as K-mesons, it may not be sufficient merely to identify particle types. Physical separation and removal of unwanted particles may be required. This is clearly true in a bubble chamber experiment requiring a K-meson beam - the thousands of superimposed pion tracks in each picture would be intolerable. A counter experiment (by this I mean one which gathers its data by means of detectors such as spark chambers, scintillation counters, Cerenkov counters, etc., which can be triggered after the identification of an incoming beam particle) encounters difficulties when the rates become so high that many wanted and unwanted particles coincide within the resolving time of the apparatus. So here too, actual physical

*Work performed under the auspices of the U.S. Atomic Energy Commission.

separation of particle types becomes desirable in order to detect rare interactions caused by the wanted particle, and it is with this type of experiment that we shall primarily be concerned here.

In order to separate an unwanted particle, we shall wish to subject it to a force which can change its original motion in a way dependent upon its velocity. Proposals have been made to do this by means of longitudinal forces, but let us here restrict the discussion to transverse forces producing an angular change in the direction of flight. First of all, we see that a simple static magnetic field will not suffice, for in this case

$$\frac{d\theta_i}{ds} = \frac{e B(s)}{p}$$

where s is the coordinate along the trajectory. Thus the deflection depends only on the momentum of the particle and, in fact, it is in this way that the momentum of the beam particles is established to begin with. In a static electric field

$$\frac{d\theta_i}{ds} = \frac{e E(s)}{p v_i}$$

for small angles of deflection. This is quite a practical solution and is employed in the many electrostatic separators now in use at various laboratories. But note that the separation, that is, the difference in angular deflection between two particle types, goes like

$$\theta_i - \theta_j \sim \frac{eE\ell}{p} \left(\frac{1}{v_i} - \frac{1}{v_j} \right)$$

where

$$\left(\frac{1}{v_i} - \frac{1}{v_j} \right) \cong \frac{1}{c} \frac{(m_i c)^2 - (m_j c)^2}{p^2}$$

Hence, the total deflecting capability of the field, $eE\ell/pv$, is reduced by the factor $(1/v_i - 1/v_j)$, which typically ranges from 0.01 to 0.001 at momenta of interest here. Thus the electrostatic separator rapidly becomes inefficient at high momenta since $\theta_i - \theta_j \propto 1/p^3$.

Considering next a time-varying electric field, we may write

$$\frac{d\theta_i}{ds} = \frac{e E(s)}{p v_i} e^{i(ws/v_i)}$$

Here, the $1/v_i$ factor in the amplitude will be unimportant at large momenta, but for high frequencies the phase ws/v_i can now be made to differ by amounts comparable to π for different particle types i . Therefore, by proper phasing, the separation angle can be on the order of $eE\ell/pv$ and it decreases only as $1/p$. Let us now turn to a practical embodiment of this idea.

II. PRACTICAL UTILIZATION OF HIGH FREQUENCY DEFLECTING FIELDS

The rf separator arrangement to be considered here was put forward by Panofsky in 1959,¹ and in its simplest form is the basis of the presently operating short pulse, room temperature separators at CERN and Brookhaven.^{2,3}

Figure 1 illustrates the principle of this method of separation. The secondary beam, with momentum p previously determined, enters a first rf resonant cavity whose transverse electric field is in the vertical direction, for example. If the cavity is relatively short, all particle types passing the cavity at time t will be deflected by an amount

$$\hat{\theta}_i = \frac{eE_i \ell}{p v_i} e^{i\omega t}$$

where eE_i is the effective transverse force acting upon the particle i during its passage through the cavity. At high momenta, if the phase velocity of the field in the cavity is close to c , then the variation of E_i is slight from one particle type to another. After traversing a distance L , which includes an imaging section to economize on aperture, the particles encounter another rf deflector whose excitation phase is ϕ with respect to the first. They are therefore left with a net angular departure from their original directions of

$$\theta_i = \frac{eE_i \ell}{p v_i} e^{i\omega t} \left[e^{i[\phi + (\omega L/v_i)]} - 1 \right].$$

In order to eliminate a certain particle type, say π 's, we choose $\phi = -\omega L/v_\pi$ so that the second deflector just cancels the effect of the first one to give $\theta_\pi = 0$. These unwanted particles then can be caused to strike an absorber or "stopper" and be removed from the beam.

With ϕ as given, another wanted particle type, K , will have a net deflection of

$$\theta_K = \left[2i \frac{eE_K \ell}{p v_K} \sin \frac{1}{2} \omega L \left(\frac{1}{v_K} - \frac{1}{v_\pi} \right) \right] e^{i\omega t} e^{i\frac{1}{2}\omega L(1/v_K - 1/v_\pi)}$$

Thus, if the relative phase slip $\omega L(1/v_K - 1/v_\pi)$ between wanted and unwanted particles is close to $(\pi \times \text{odd integer})$, the wanted ones will emerge with approximately twice the deflection amplitude of a single cavity. Many of them will be able to pass easily above or below the edges of the absorber mentioned above and proceed into the experimental apparatus. Of course, a fraction of the wanted particles which traverse the cavities when the fields are near zero will strike the stopper and be lost. The criterion for best π - K separation then is

$$\frac{L}{\lambda} \left(\frac{1}{\beta_K} - \frac{1}{\beta_\pi} \right) = n + \frac{1}{2}; \quad \{n = 0, 1, 2, \dots\}$$

1. See, for example, B.W. Montague, Progr. Nucl. Techn. & Instr. (North-Holland Publishing Co., 1968), Vol. 3, p. 3.

2. W. Schnell, Report CERN 61-5 (1961).

3. H. Hahn, H.J. Halama, and H.W.J. Foelsche, Brookhaven National Laboratory, Accelerator Dept. Report AADD-91 (1965).

where λ is the free space wavelength corresponding to the excitation frequency ω of the cavities, and $\beta_i = v_i/c$.

Now in a beam of positively charged particles, there are copious quantities of protons as well as pions. In this case it would be desirable to eliminate protons as well to obtain a more pure K^+ beam. By changing subscript K to subscript p, we see that

$$\theta_p = \left[2i \frac{eE_p \ell}{p v_p} \sin \frac{1}{2} \omega L \left(\frac{1}{v_p} - \frac{1}{v_\pi} \right) \right] e^{i\omega t} e^{i\frac{1}{2}\omega L(1/v_p - 1/v_\pi)}$$

It is clear that θ_p can be made zero too (we have already required $\theta_\pi = 0$) if the π -p relative phase slip is ($2\pi \times \text{integer}$). Hence, to reject both pions and protons (double rejection):

$$\frac{L}{\lambda} \left(\frac{1}{\beta_p} - \frac{1}{\beta_\pi} \right) = n ; \quad \{n = 1, 2, 3, \dots\}$$

Figure 2 is a plot of net deflection amplitude after the second cavity as a function of relative momentum (p/p_0). Here, p_0 has been chosen as the highest momentum at which double (π -p) rejection is obtained. Hence, the curve labeled π -p goes to zero at $(p/p_0) = 1$. Although, for definiteness, it has been assumed that pions were to be eliminated, this curve applies equally well if protons are the unwanted particle. The only difference will lie in the empirically tuned phase difference ϕ between the two cavities. Maximum kaon deflection, on the same momentum scale, then occurs near $(p/p_0) = 0.7$. It should be noted that the net deflection amplitude has been normalized by the factor $eE\ell/pc\beta$, i.e., by the deflection amplitude of a single cavity, which varies as $1/p$. Hence the absolute deflection amplitude actually obtained would be (p_0/p) times the ordinate of the appropriate curve.

III. PROPOSED ENRICHED PARTICLE BEAM

As stated above, the primary concern here is the use of rf cavities to produce separated, or at least enriched, particle beams for use by counter experiments. Because of the limitations encountered due to high flux rates, the duration of the beam entering the detectors must be as long and uniform as possible. Here at the AGS this duration is as much as 0.5 sec out of each 2.4 sec, the common repetition period of the accelerator. It is for this reason that superconducting cavities become attractive, since the rf source required for the very high average power level of a room temperature cavity would be a formidable problem. For example, this might amount to $10 \text{ MW} \times 0.5/2.4 = 2 \text{ MW}$ average power.

For the initial employment of long pulse, superconducting separators at Brookhaven, we propose to utilize the relatively simple two-cavity arrangement outlined above.⁴ The complete beam may conveniently be divided into four sections:

1. Source emittance definition - momentum band, transverse phase space.
2. Angular separation.
3. Purification.
4. Matching to detector.

As indicated in Fig. 3, sections 1 and 2 are distinct, in the present arrangement, but 3 and 4 overlap.

4. H. Hahn and H.J. Halama, IEEE Trans. Nucl. Sci. NS-14, No. 3, 356 (1967).

1. Source Emittance Definition

Before defining the source, the admittance of the separation section must be examined. As we have seen, for a given separation condition and momentum (e.g., double π -p rejection at 16 GeV/c), the interdeflector length L is proportional to the wavelength (e.g., $L = 593 \lambda$ for the cited condition). Since our experimental space is not unlimited, we have foregone the gain in flux possible by using large aperture, low frequency cavities,⁴ and have chosen the S-band frequency to shorten the beam length and benefit from the easy availability of rf sources and instrumentation in that range. Hence, $\lambda = 10.5$ cm and we have assumed a conservative iris aperture of $2a = 0.4 \lambda = 4.2$ cm.

As is commonly done, we restrict the beam in the deflectors to lie within the square circumscribed by the iris aperture to avoid scattering from the edges. Assuming a cavity length of 3 m, we then have the phase-space admittance diagram shown in Fig. 4 for the first deflector. The maximum area fillable by a simple optical system is 14.7 cm·mrad in the horizontal plane. In the vertical plane, the maximum usable admittance is set by the maximum cavity deflection and the desired separation ratio, that is, the ratio of the deflection amplitude to the intrinsic angular spread in the beam at the cavity. The expected transverse impulse imparted by the cavity is about 12 MeV/c. Hence, the deflection amplitude expected is about 0.6 mrad at a momentum of 20 GeV/c. Since we wish to use the enriched beam over a wide momentum range, the separation conditions will not always be optimum, so it would seem advisable to keep the angular width of the beam small. If this is taken as 0.5 x deflection amplitude, the resulting phase space available is 0.75 cm·mrad. These admittance areas provide bounds to be considered in designing the source emittance section. Again:

$$\begin{aligned} A_H &< 14.7 \text{ cm}\cdot\text{mrad} \\ A_V &\cong 0.75 \text{ cm}\cdot\text{mrad} \end{aligned} .$$

This beam would be constructed from a target in the slow external beam of the AGS, with its axis at an angle of 0° with respect to the primary protons. The target will be assumed to be 0.25 cm square. The separator admittances therefore indicate maximum acceptance angles at the target of

$$\left. \begin{aligned} \Delta x'_t &= 59 \text{ mrad} \\ \Delta y'_t &= 3.0 \text{ mrad} \end{aligned} \right\} \text{ full width} .$$

It has turned out to be difficult to achieve the full horizontal acceptance. Figure 5 illustrates the source definition section which employs a doublet composed of three N3Q36 quadrupoles immediately following the target to produce a "parallel" beam in both planes at the first turning point. With this arrangement

$$\left. \begin{aligned} \Delta x'_t &= 26 \text{ mrad} \\ \Delta y'_t &= 3.0 \text{ mrad} \end{aligned} \right\} \Delta\Omega = 78 \mu\text{sr} \quad \left. \begin{aligned} f_H &= 0.975 \text{ m} \\ f_V &= 8.71 \text{ m} \end{aligned} \right\} \text{ at central momentum} ,$$

where f_H and f_V are the horizontal and vertical focal lengths into the bending magnets D1 and D2.

These first two bending magnets, (D1, D2), cause a momentum dispersion which is cancelled by focusing this first turning point upon a second identical point of dispersion at (D3, D4) by the use of four 8Q48 and two 8Q24 quadrupoles. The momentum band passed is determined before dispersion cancellation by a momentum slit at the horizontal target image between the two turning points. The spatial dispersion there is 0.5 cm/%. It is planned to employ a momentum band of up to $\Delta p/p = 5\%$ full width.

At the first deflector, immediately following (D3, D4), the optical system has again produced a parallel beam with the same horizontal focal length, target into deflector, as before, $f_H = 0.975$ m.

Vertically, an image of the target is also formed at the momentum slit position, so that a slit there can redefine the vertical width of the source. This slit then also sets the angular width of the "parallel" beam in the first deflector:

$$\begin{aligned} f_v \text{ mom. slit} \rightarrow \text{RF1} &= 18.2 \text{ m} \\ f_v \text{ target} \rightarrow \text{RF1} &= 8.7 \text{ m} \end{aligned}$$

Thus, with the inclusion of a suitable solid angle defining aperture between Q2 and Q3, the emittance of the source definition section is

$$\begin{aligned} \Delta x_{\text{RF1}} &= 2.5 \text{ cm} & \Delta y_{\text{RF1}} &= 2.6 \text{ cm} \\ \Delta x'_{\text{RF1}} &= 2.6 \text{ mrad} & \Delta y'_{\text{RF1}} &= 0.3 \text{ mrad} \end{aligned}$$

at the central momentum. For off-momentum rays, the chromatic aberration in the horizontal plane is rather pronounced, and so to control the illumination of the iris edges it will be advisable to mask them with an aperture near the point which is imaged onto the cavity (this mask could be at the exit of D2). In addition, a mask should be placed immediately in front of RF1.

2. Angular Separation Section

The admittance to the first cavity has been discussed. The next parameter to be fixed is the interdeflector spacing. This has been taken as the shortest distance which will allow double π -p rejection from a K-meson beam at 16.0 GeV/c:

$$\frac{L}{\lambda} = \frac{1}{\left(\frac{1}{\beta_p} - \frac{1}{\beta_\pi}\right)} \doteq \frac{1}{(m_p c)^2 - (m_\pi c)^2} = 592.8$$

$$L = 62.24 \text{ m (for } \lambda = 10.5 \text{ cm) .}$$

As assumed earlier, since the cavities are identical, the deflected particle at RF1 is to be refocused upon the second deflector RF2 with a magnification of -1. As has become common practice, in order to reproduce the phase space of RF1 in RF2 to avoid beam loss, the complete transform between the two cavities has been made equal to the negative unity transform in both planes. (Though not strictly necessary now in the horizontal plane, it will be more important if future improvements allow the RF1 admittance area to be filled more completely.) The optical arrangement chosen for this is a symmetrical sextuplet of 8Q48 quadrupoles shown in Fig. 6. The sextuplet seems to require less power than the quadruplet solution would. It has the added advantages of double horizontal and vertical imaging at the center, which makes instrumentation for focusing the beam simpler, and the transform matrix element $V_{22} = -1$, which determines the slope of the deflected particle at RF2, does not depend on momentum to first order.

Referring to Fig. 2, the approximate ranges in momentum available for different particle types have been estimated and are shown in Fig. 7. The dotted lines indicate extended ranges which may be possible if one can tolerate higher impurities. For instance, good K^+ enrichment is obtained only in rather narrow bands, but if single rejection of π^+ or p^+ proves to be sufficient the larger K^- range can be covered.

There are three imperfections in the angular separation section which should be considered. The first is the chromatic aberration in the interdeflector optics. The most important term in the vertical transform matrix is $V_{22} \cong -1 + 5.6 (\delta p/p)^2$ plus higher order terms, as mentioned previously. (In fact, this is true of V_{11} also.) Because of this, the cancellation of the pion deflection, for example, is unimpaired. The off-diagonal terms depend on the first power of $(\delta p/p)$ and cause some mismatch with the admittance of the second deflector, but the loss and scattering from the cavity irises is not serious.

The second possible source of error in phasing of the unwanted particles is due to the increased path length, δL , of off-axis rays in the interdeflector region. Since an increment of path length is

$$ds + (dx^2 + dy^2 + dz^2)^{\frac{1}{2}} = (1 + x'^2 + y'^2)^{\frac{1}{2}} dz \cong dz + \frac{1}{2} (x'^2 + y'^2) dz ,$$

δL may be expressed as

$$\delta L \cong \frac{1}{2} \int_0^L (x'^2 + y'^2) dz .$$

The extreme rays in this beam have

$$\delta L \leq 0.0025 L .$$

This is not serious. For double π -p rejection with $n = 2$ (i.e., 4π phase slip between pions and protons), this corresponds to a phase error of 1.8° and a maximum net deflection error of $\sim 3\%$ of the single cavity amplitude.

Phase error due to velocity differences within the transmitted momentum band are the most serious. The change in deflection amplitude θ_i (in terms of unit single cavity deflection) is

$$\delta\theta_i \cong - \left[\pi \frac{L}{\lambda} \frac{(m_i c)^2}{p} \beta_i \cos \frac{1}{2} \left(\frac{2\pi L}{\lambda \beta_i} + \varphi \right) \right] \frac{\delta p}{p} ,$$

which is clearly largest for protons ($m_i = m_p$). At double π -p rejection,

$$\delta\theta_p \cong 2\pi n \left(\frac{m_p^2}{m_p^2 - m_\pi^2} \right) \beta_p \frac{\delta p}{p} .$$

Table I illustrates the effect of this error on the effective separation ratio for the first three double π -p rejection points.

TABLE I

n =	1	2	3
p (GeV/c)	16.0	11.2	9.3
θ_K (mrad)	0.65	1.28	1.00
η_0	2.2	4.3	3.3
$\delta\theta_p$ (mrad)	0.12	0.34	0.62
$(\Delta y')_{\text{prot.}}$ (mrad)	0.42	0.64	0.92
$\eta_{\text{eff.}}$	1.6	2.0	1.1

In the table, θ_K is the net kaon deflection, η_0 the nominal separation factor ($\theta_K/0.3$ mrad), $\Delta y'_{\text{prot.}}$ the increased angular width of the proton beam at the second deflector ($\Delta y'_{\text{prot.}} = 0.3 + \delta\theta_p$ mrad, a liberal estimate), and $\eta_{\text{eff.}}$ the effective separation ratio of kaons from protons.

3. Purification Section

The angularly separated beam from RF2 is focused in both planes onto the stopper located at the focal plane of the doublet (Q16, Q17) of Fig. 8. This doublet has $f_H = 5.1$ m and $f_V = 18.0$ m. A 50 cm length of Hevimet will cause about 90% of any undeflected, unwanted particles hitting it to suffer inelastic collisions and the rest, through ionization, will lose 1.2 GeV or more in energy. Thus, unwanted particles will lose 6% or more in momentum and be scattered, on the average, by 8 mrad or more. A momentum-dispersive system can then separate the wanted particles, with $\Delta p/p = 5\%$, from the unwanted particles 6% lower in momentum if the system has a suitable momentum separation ratio, i.e., if the intrinsic beam width corresponds to, say, 2% or less in momentum. The dispersive section may also have an aperture closely matched to the wanted beam so that some unwanted particles are removed quickly as a result of scattering in the stopper.

The rest of the purification section thus consists of an arrangement with $f_H = 18$ m into the two bending magnets (D5, D6) and out again ($f_H = 18.0$ m) to the next horizontal focus where the final momentum slit is located. There is also a second stopper here upon which any stubborn vertically focused unwanted particles can be eliminated. The two vertical focal lengths are each 5.1 m.

4. Matching Section

As an example, a matching section is included which brings the beam at the end into essentially the same vertical phase space it occupied in RF2, namely $\Delta y = 2.5$ cm and $\Delta y' = 0.3 + 2$ mrad or so depending on final net deflections at RF2. There is no "hole" in the spatial distribution. Horizontally the spatial momentum dispersion $\partial x/\partial p$ is zero, but an angular dispersion remains. It amounts to about a 15-mrad spread. If objectionable, a final set of bending magnets would be required to remove it. The horizontal extent here is about 2.5 cm as in RF2.

IV. FLUX ESTIMATES

As an example of particle fluxes in this beam, the π^- , K^- , and \bar{p} yields at the end are shown as a function of momentum in Fig. 9. These curves are based on the empirical curves of Sanford and Wang.⁵ They have not been corrected for stopper losses. The efficiency of passage around the stopper varies with the separation factor η_M approximately as shown in Fig. 10. This is the result of assuming that the vertical distribution at the stopper is trapezoidal and that the stopper just covers its base width.

V. PRIMARY PROTON DUMP

In the beam design just described, the primary protons which do not interact in the target pass through the first quadrupoles into the bending magnets D1 and D2. If these magnets should be set for positive secondaries of 6.5 to 20 GeV/c, the 28 GeV/c

5. J.R. Sanford and C.L. Wang, Brookhaven National Laboratory, Accelerator Dept. Reports JRS/CLW-1 and JRS/CLW-2 (1967).

(assumed) primaries would pass through and be dumped in an absorber between D2 and Q4. For a negative secondary beam, the dump occurs mostly inside D2. The situation can be helped by offsetting D2 laterally to allow more of the primaries to pass through, but nevertheless the aperture of D2 would have to be packed with absorber to reduce the irradiation of its copper coils as much as possible.

VI. AREAS FOR IMPROVEMENT

An increased solid angle accepted by the beam would be helpful. In principle, the rf cavities would allow up to 180 μ sr, using the same 0.25 cm square target assumed. This much would probably be difficult to obtain, but a factor of two increase may be possible. In doing so, the total beam length should not be increased very much, and standard magnet types should be employed.

Although the maximum momentum band of 5% seems to be a reasonable one to retain, improved flexibility would result if the momentum separation factor η_p could be increased. At present it is equal to unity at $\Delta p/p = 2.5\%$, which is, therefore, the lower limit on the momentum band. A smaller target, say 0.1 cm, would reduce this to 1.0%, but it would be attractive to get to even lower values, say 0.5 to 0.25%, for certain experiments which might require it. The need for this can sometimes be circumvented by operating with the full 5% band but defining the momenta of individual particles in the enriched beam by employing hodoscopes or wire plane chambers in conjunction with the momentum analysis done in the purification section. Here again, an improved momentum resolution would be needed. As before, we would prefer to keep the beam length to a minimum.

The primary proton beam dumping situation is not ideal. Further investigation should be done to determine if these protons could be absorbed in a place more removed from beam components.

VII. SUMMARY OF BEAM PARAMETERS

Momentum	16 GeV/c for π -p rejection 20 GeV/c maximum
Momentum band	$\pm 1.25\%$ to $\pm 2.5\%$
Acceptance angles	± 13 mrad horizontal, at p_0 ± 1.5 mrad vertical, at p_0
Solid angles	78 μ sr at p_0 56 μ sr over 5% momentum band
Length, primary to secondary target	162 m
Cavity frequency	2.865 GHz
Iris aperture	4.1 cm diam
Cavity length	3 m
Transverse impulse	12 MeV/c
Number of rf cavities	2
Interdeflector separation	62 m
Magnet complement	3 - N3Q36 6 - 8Q24 16 - 8Q48 6 - 18D72

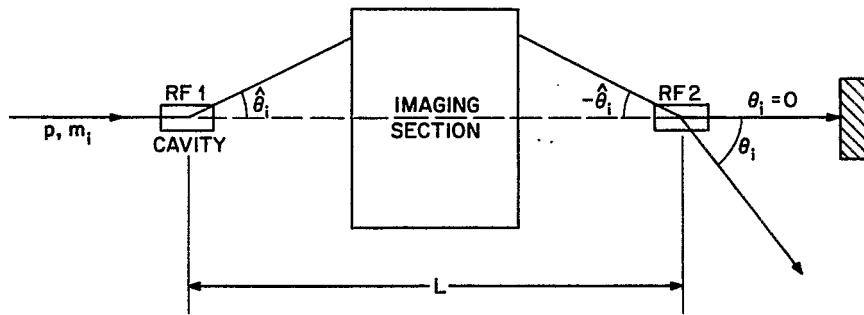


Fig. 1. Schematic rf separation.

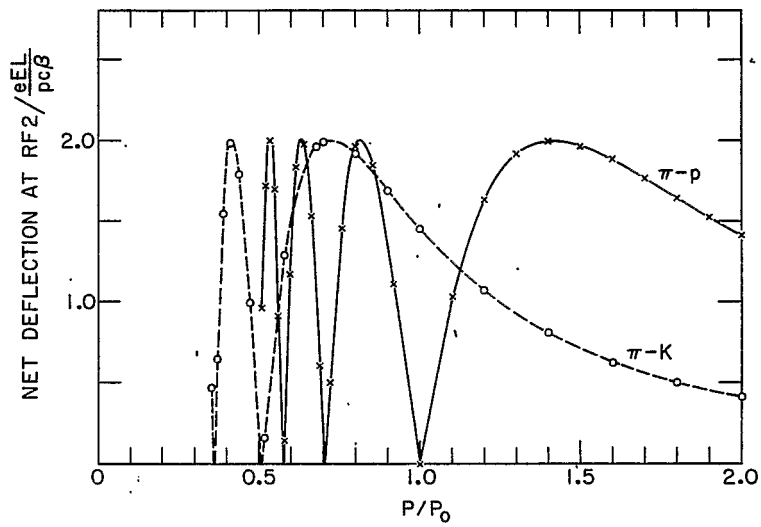


Fig. 2. Net deflection amplitudes following a two-cavity separator vs momentum.

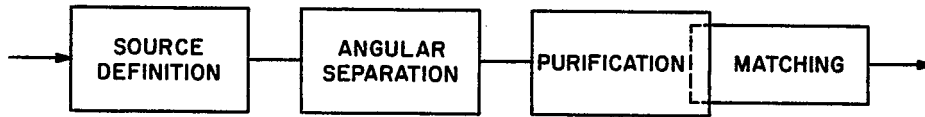


Fig. 3. Block diagram of proposed beam.

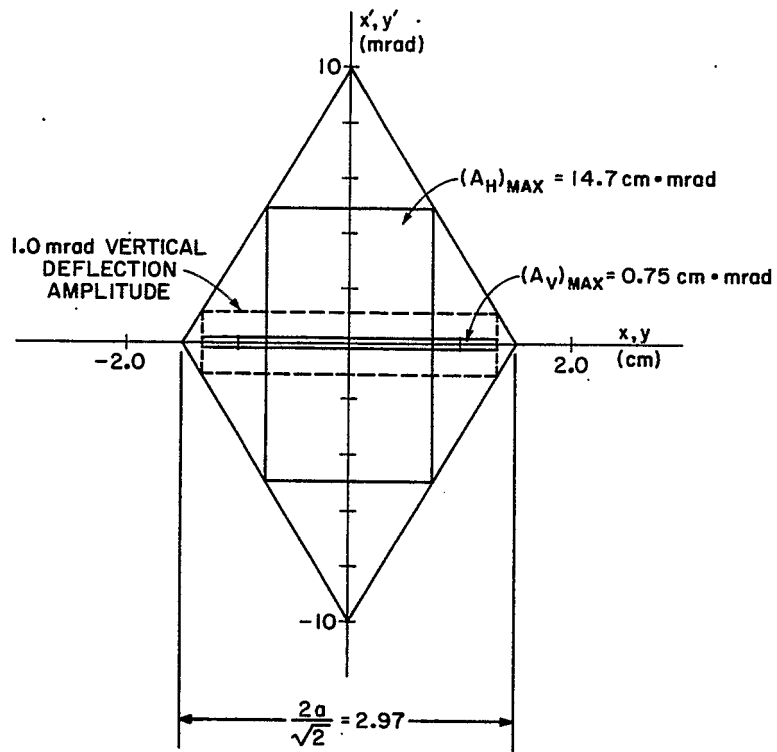


Fig. 4. Rf cavity admittance diagram.

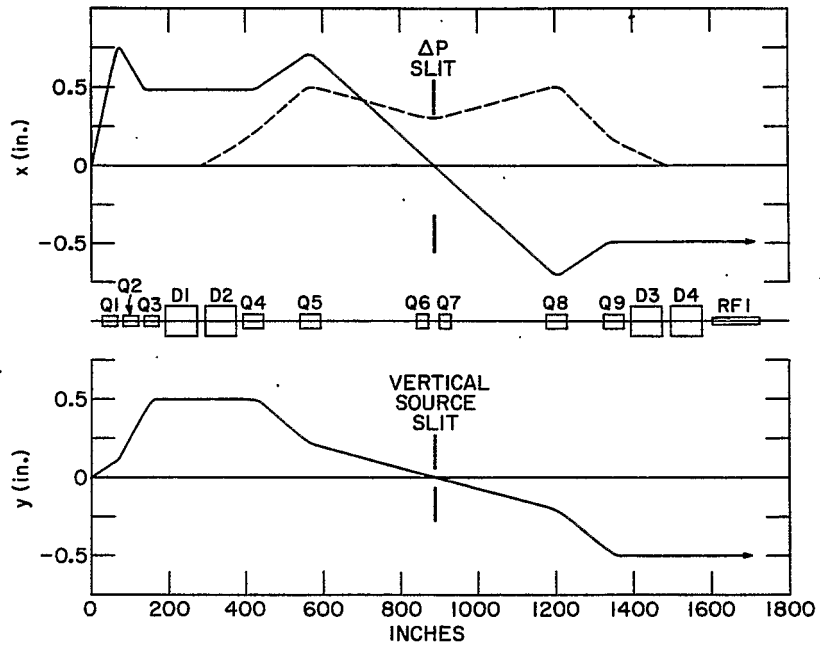


Fig. 5. Component layout and ray trace for source definition section.

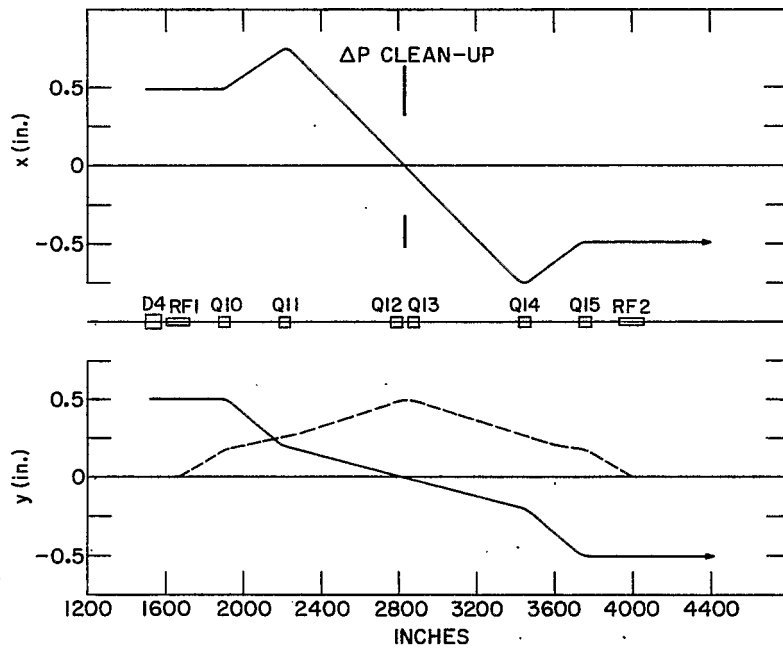


Fig. 6. Component layout and ray trace for interdeflector section.

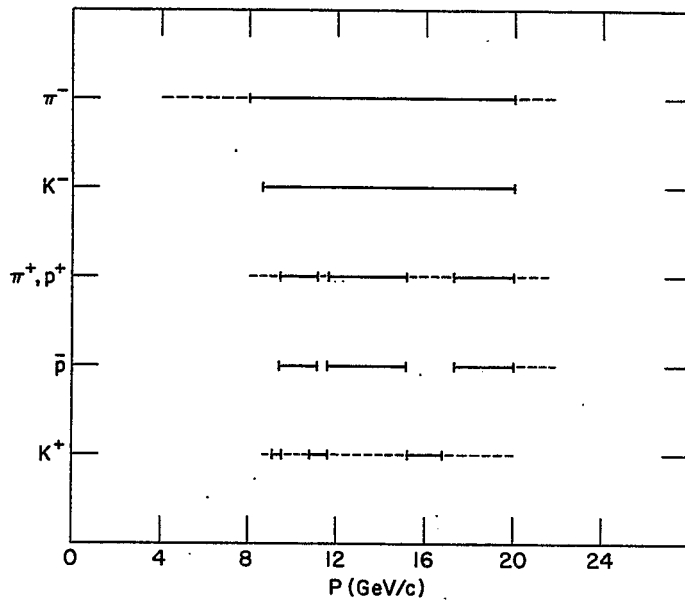


Fig. 7. Operating momentum ranges.

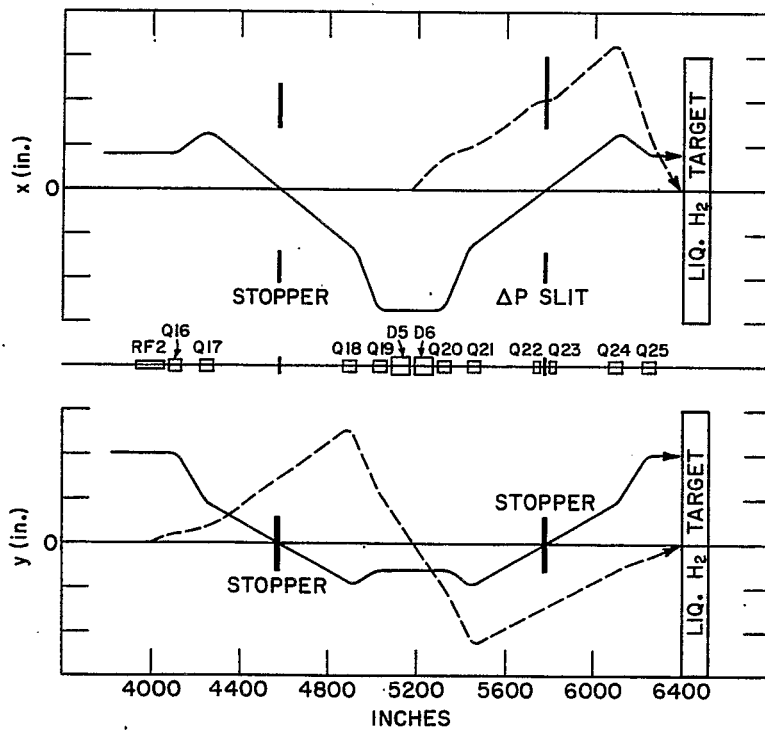


Fig. 8. Component layout and ray trace for purification and matching section.

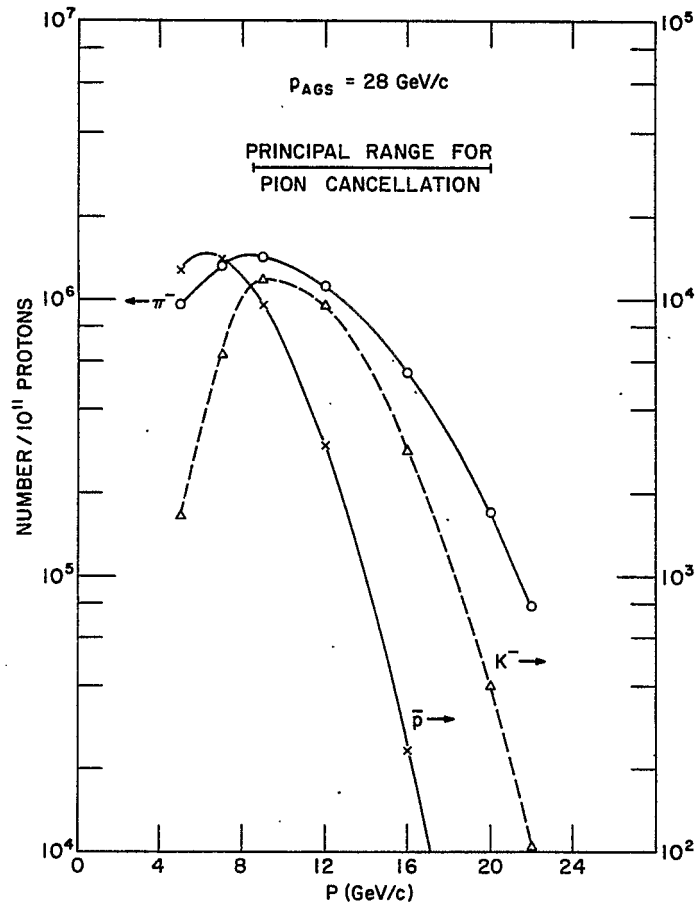


Fig. 9. Particle fluxes at end of beam (stopper passage efficiency not included).

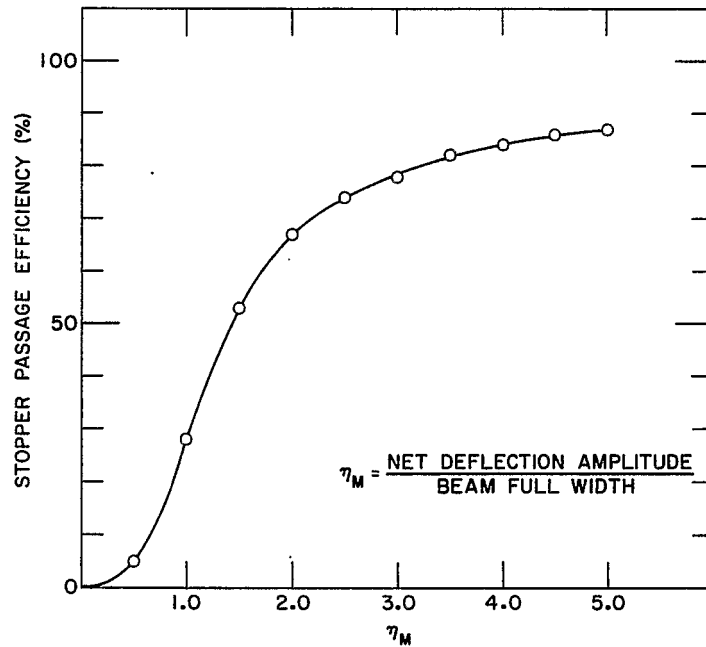


Fig. 10. Stopper passage efficiency vs momentum.